THE JOURNAL OF BIOLOGICAL CHEMISTRY Vol. 277, No. 7, Issue of February 15, pp. 5047–5053, 2002
Printed in U.S.A.

The Molecular Basis of Glycogen Storage Disease Type 1a

STRUCTURE AND FUNCTION ANALYSIS OF MUTATIONS IN GLUCOSE-6-PHOSPHATASE*

Received for publication, October 31, 2001
Published, JBC Papers in Press, December 5, 2001, DOI 10.1074/jbc.M110486200

Jeng-Jer Shieh, Mugen Terzioglu, Hisayuki Hiraiwa, Julia Marsh, Chi-Jiunn Pan, Li-Yuan Chen, and Janice Yang Chou‡

From the Heritable Disorders Branch, NICHD, National Institutes of Health, Bethesda, Maryland 20892

Glycogen storage disease type 1a is caused by a deficiency in glucose-6-phosphatase (G6Pase), a nine-helical endoplasmic reticulum transmembrane protein required for maintenance of glucose homeostasis. To date, 75 *G6Pase* mutations have been identified, including 48 mutations resulting in single-amino acid substitutions. However, only 19 missense mutations have been functionally characterized. Here, we report the results of structure and function studies of the 48 missense mutations and the ΔF327 codon deletion mutation, grouped as active site, helical, and nonhelical mutations. The 5 active site mutations and 22 of the 31 helical mutations completely abolished G6Pase activity, but only 5 of the 13 nonhelical mutants were devoid of activity. Whereas the active site and nonhelical mutants supported the synthesis of G6Pase protein in a manner similar to that of the wild-type enzyme, immunoblot analysis showed that the majority (64.5%) of helical mutations destabilized G6Pase. Furthermore, we show that degradation of both wild-type and mutant G6Pase is inhibited by lactacystin, a potent proteasome inhibitor. Taken together, we have generated a data base of residual G6Pase activity retained by G6Pase mutants, established the critical roles of transmembrane helices in the stability and activity of this phosphatase, and shown that G6Pase is a substrate for proteasome-mediated degradation.

Glycogen storage disease type 1 (GSD-1),[1] also known as von Gierke disease, is a group of autosomal recessive metabolic disorders that occur approximately once in every 100,000 live births (reviewed in Refs. 1–3). GSD-1a (MIM 232 200), the major subtype representing over 80% of GSD-1 cases, is caused by a deficiency in glucose-6-phosphatase (G6Pase; EC 3.1.3.9), which catalyzes the hydrolysis of glucose-6-phosphate to glucose and phosphate, the terminal steps in gluconeogenesis and glycogenolysis. Patients afflicted with GSD-1a cannot maintain glucose homeostasis and manifest hypoglycemia, hepatomegaly, kidney enlargement, growth retardation, hyperlipidemia, hyperuricemia, and lactic acidemia. Long-term complications include gout, hepatic adenomas with risk for malignancy, osteoporosis, platelet dysfunction, pulmonary hypertension, and renal failure.

The cloning of the *G6Pase* gene has enabled researchers to show that GSD-1a individuals are homozygotes or compound heterozygotes for loss of function mutations in the gene (4–11). To date, 75 *G6Pase* mutations (including 2 reported here) have been identified in GSD-1a patients on the basis of their absence from the normal population and/or their co-segregation with the disease phenotype (reviewed in Refs. 2 and 3). Interestingly, 48 candidate mutations are missense mutations that result in single-amino acid substitutions. Characterization of these mutations will provide critical information on functionally important residues of the protein. In this study, we functionally characterize all 48 missense mutations by site-directed mutagenesis and transient expression assays. A data base of residual enzymatic activity retained by the G6Pase mutants will serve as a reference for evaluating genotype-phenotype relationships and the minimal G6Pase activity required to correct the GSD-1a phenotype.

Sequence alignment suggests that mammalian G6Pases, lipid phosphatases, acid phosphatases, and vanadium haloperoxidases share a conserved phosphatase signature motif, and in G6Pase, this occurs between residues 76 and 180 (12, 13). The crystal structure of the vanadium-containing chloroperoxidase from the plant pathogenic fungus *Curvularia inaequalis* has been resolved (14). The results show the active site residues in vanadium-containing chloroperoxidase are contained within the phosphatase signature motif. Based on the crystal structure and mechanism of action of vanadium-containing chloroperoxidase (13, 14), the amino acids predicted to participate in G6Pase catalysis include Lys^{76}, Arg^{83}, His^{119}, Arg^{170}, and His^{176}. Five mutations that alter active site residues in G6Pase, K76N, R83C, R83H, H119L, and R170Q, have been identified in GSD-1a patients (4, 6, 15–17). R83C and R83H were shown to abolish phosphatase activity in transient expression assays (4, 6). In this study, we show that K76N, H119L, and R170Q also completely abolish G6Pase activity, demonstrating the importance of these residues in G6Pase catalysis.

Very little is known about the structural requirements for the correct folding and catalytic activity of G6Pase. We have shown that human G6Pase is anchored to the endoplasmic reticulum (ER) by nine transmembrane helices with the amino terminus in the lumen and the carboxyl terminus in the cytoplasm (18, 19). Therefore, the large collection of G6Pase mutations can now be studied in the context of their positions with respect to the ER and the cytoplasm. In this study, we undertake structure-function analysis of G6Pase. We show that amino acid residues that comprise the catalytic center and nonhelical regions in G6Pase play no essential role in the stability of the enzyme. On the other hand, the structural integrity of transmembrane helices is critical for the correct folding, stability, and enzymatic activity of G6Pase.

* The costs of publication of this article were defrayed in part by the payment of page charges. This article must therefore be hereby marked "*advertisement*" in accordance with 18 U.S.C. Section 1734 solely to indicate this fact.

‡ To whom correspondence should be addressed: Bldg. 10, Rm. 9S241, Heritable Disorders Branch, NICHD, National Institutes of Health, Bethesda, MD 20892-1830. Tel.: 301-496-1094; Fax: 301-402-6035; E-mail: chou@helix.nih.gov.

[1] The abbreviations used are: GSD-1, glycogen storage disease type 1; G6Pase, glucose-6-phosphatase; WT, wild-type; ER, endoplasmic reticulum.

Proteins with abnormal conformation are rapidly eliminated through intracellular protein degradation, which represents a quality control system in cells (20). Cytosolic proteasomes are responsible for rapid degradation of many membrane proteins, including cystic fibrosis transmembrane conductance regulator (21, 22), the major histocompatibility complex class I molecule, and the α-chains of T-cell antigen receptor (reviewed in Refs. 23–25). The proteasome pathway can be inhibited by the *Streptomyces* metabolite, lactacystin (26), which inhibits the proteasome specifically without inhibiting other proteases (reviewed in Ref. 27). The availability of proteasome inhibitor allows a rapid analysis in intact cells of the possible contributions of protein breakdown by the proteasomes. In this study, we show that wild-type and mutant G6Pases are predominantly degraded in the ER through the proteasome pathway.

MATERIALS AND METHODS

Mutational Analysis—The *G6Pase* gene in GSD-1a patients was characterized by single-strand conformational polymorphism analysis (28) on mutation detection enhancement gels (AT Biochem, Malvern, PA) containing 5% glycerol. Exon-containing fragments were amplified by PCR using primers containing intronic, 5′-, and 3′-untranslated sequences of the human *G6Pase* gene as described previously (6). The mutation-containing fragments identified by single-strand conformational polymorphism analysis were subcloned and characterized by DNA sequencing.

Construction of G6Pase Mutants and Expression in COS-1 Cells—Human G6Pase-*Dra*III (29) cDNA was used as a template for mutant construction by PCR. The eight-amino acid FLAG marker peptide, DYKDDDDK (Scientific Imaging Systems, Eastman Kodak, CT) was used to tag the amino or carboxyl terminus of G6Pase as described previously (18). The two outside PCR primers for G6Pase mutants that contain mutations upstream of the *Dra*III site are nucleotides 77–96 (G1; sense) and nucleotides 625–602 of G6Pase-*Dra*III (I2; antisense) (29), and the two outside PCR primers for mutants that contain mutations downstream of the *Dra*III site are nucleotides 611–634 (I1; sense) and nucleotides 1150–1133 of *G6Pase-Dra*III (G2; antisense). The two outside primers for G6Pase R170Q, G184E, G184V, G188D, and G188R mutants are G1 and G2. After PCR, the amplified fragment was ligated into either the pSVLhG6Pase-*Dra*III-3′ fragment, the pSVLhG6Pase-*Dra*III-5′ fragment, or the pSVL fragment.

The mutant primers are: M5R (nucleotides 83–103), ATG→A**G**G at position 5; T16A (nucleotides 116–136), ACA→**G**CA at position 16; Q20R (nucleotides 128–148), CAG→C**G**G at position 20; Q54P (nucleotides 230–250), CAG→C**C**G at position 54; W63R (nucleotides 257–277), TGG→**C**GG at position 63; G68R (nucleotides 272–292), GGA→**C**GA at position 68; K76N (nucleotides 296–316), AAG→AA**C** at position 76; W77R (nucleotides 299–319), TGG→**C**GG at position 77; G81R (nucleotides 311–331), GGA→**C**GA at position 81; T108I (nucleotides 392–412), ACC→A**T**C at position 108; T111I (nucleotides 401–421), ACT→A**T**T at position 111; P113L (nucleotides 407–427), CCA→C**T**A at position 113; H119L (nucleotides 425–445), CAT→C**T**T at position 119; G122D (nucleotides 434–454), GGC→G**A**C at position 122; A124T (nucleotides 440–460), GCA→**A**CA at position 124; W156L (nucleotides 535–555), TGG→**T**TG at position 156; V166A (nucleotides 566–586), GTC→G**C**C at position 166; R170Q (nucleotides 578–598), CGA→C**A**A at position 170; H179P (nucleotides 605–625), CAT→C**C**T at position 179; G184E (nucleotides 620–640), GGA→G**A**A at position 184; G184V (nucleotides 620–640), GGA→G**T**A at position 184; G188D (nucleotides 632–652), GGC→G**A**C at position 188; G188R (nucleotides 632–652), GGC→**C**GC at position 188; L211P (nucleotides 701–721), CTC→C**C**C at position 211; A241T (nucleotides 791–811), GCC→**A**CC at position 241; T255I (nucleotides 833–853), ACC→A**T**C at position 255; P257L (nucleotides 839–859), CCC→C**T**C at position 257; N264K (nucleotides 860–880), AAC→AA**A** at position 264; L265P (nucleotides 863–883), CTG→C**C**G at position 265; G266V (nucleotides 866–886), GGC→G**T**C at position 266; G270R (nucleotides 878–898), GGC→**C**GC at position 270; S298P (nucleotides 962–982), TCT→**C**CT at position 298; F322L (nucleotides 1034–1054), TTC→**C**TC at position 322; V338F (nucleotides 1082–1102), GTC→**T**TC at position 338; and I341N (nucleotides 1091–1111), ATC→AA**C** at position 341. The antisense primer for each mutant has the corresponding complementary sequence. *Bold letters* indicate nucleotide changes. We have also constructed carboxyl-terminal FLAG-tagged human G6Pase mutants, R83C, R83H, E110K, E110Q, V166G, G188S, G222R, W236R, G270V, R295C, ΔF327, and L345R, as described previously (4–6). The nucleotide sequence in all constructs was verified by DNA sequencing. D38V-3′-FLAG and P178S-3′-FLAG mutants have been described previously (19).

COS-1 cells were grown at 37 °C in HEPES-buffered Dulbecco's modified minimal essential medium supplemented with 4% fetal bovine serum. Cells in 25-cm^2 flasks were transfected with 10 μg of wild-type (WT) or mutant construct in a pSVL vector by the DEAE-dextran/chloroquine method as described previously (30). To correct for transfection efficiency, 2 μg of pCMVβ (BD Biosciences, CLONTECH) was cotransfected with WT or mutant G6Pase cDNA construct. After incubation at 37 °C for 2 days, the transfected cultures were harvested for phosphohydrolase and β-galactosidase assays, Western blot analysis, or RNA isolation.

Phosphohydrolase and β-Galactosidase Assays—Phosphohydrolase activity was determined essentially as described previously (4). Reaction mixtures (100 μl) contained 50 mM cacodylate buffer, pH 6.5, 10 mM glucose-6-phosphate, 2 mM EDTA, and appropriate amounts of cell homogenates and were incubated at 30 °C for 10 min. Sample absorbance was determined at 820 nm and is related to the amount of phosphate released using a standard curve constructed by a stock of inorganic phosphate solution. Nonspecific phosphatase activity was estimated by preincubating cell homogenates at pH 5 for 10 min at 37 °C, a condition that inactivates the thermolabile G6Pase (31).

β-Galactosidase activity was measured by the release of *O*-nitrophenol from *O*-nitrophenyl-β-galactopyranoside at 37 °C in a reaction mixture containing 100 mM sodium phosphate buffer, pH 7.3, 1 mM $MgCl_2$, 50 mM β-mercaptoethanol, and 0.665 mg/ml *O*-nitrophenyl-β-galactopyranoside. β-Galactosidase activity was estimated by absorbance at 420 nm using a β-galactosidase standard obtained from Promega Biotech.

Northern Blot, Western Blot, and in Vitro Transcription-Translation Analyses—Total RNA was isolated using the RNeasy total RNA isolation kit (Qiagen), fractionated by electrophoresis through a 1.2% agarose gel containing 2.2 M formaldehyde, and transferred to a Hybond-N+ membrane (Amersham Biosciences, Inc.) by electroblotting. The membranes were hybridized with either a G6Pase or β-actin probe labeled by random priming.

For Western blot analysis of FLAG-tagged G6Pase, proteins in transfected COS-1 lysates were separated by electrophoresis through a 13% polyacrylamide-SDS gel and trans-blotted onto polyvinylidene fluoride membranes (Millipore). The membranes were first incubated with a monoclonal antibody against the FLAG epitope (Scientific Imaging Systems) and then incubated with goat anti-mouse IgG antibody (Kirkegarrd & Perry Laboratories, Gaithersburg, MD). The immunocomplex was detected with the horseradish peroxidase-linked chemiluminescence system containing the SuperSignal West Pico Chemiluminescent substrate obtained from Pierce.

In vitro transcription-translation of G6Pase cDNA constructs in a pGEM-11Zf(+) vector was performed using the troponin T-coupled reticulocyte lysate system obtained from Promega Biotech (Madison, WI). L-[^{35}S]methionine was used as the labeled precursor. The *in vitro* synthesized proteins were analyzed by 12% polyacrylamide-SDS gel electrophoresis and fluoro-autoradiography.

RESULTS

Mutations Identified in the G6Pase Gene of GSD-1a Patients—Single-strand conformational polymorphism and DNA sequencing analyses were used to identify mutations in the *G6Pase* gene of four GSD-1a patients. Six different mutations were identified, including T255I, 158delC, 836delA, W70X, Q347X, and ΔF327 (Table I). Two novel mutations identified in this study are T255I and 836delA.

G6Pase Mutations That Cause GSD-1a—Characterization of missense mutations that result in single-amino acid substitutions will provide valuable information on functionally important residues in G6Pase. The 48 missense *G6Pase* mutations identified in GSD-1a patients are scattered throughout the primary sequence (Fig. 1). Nineteen missense mutations, including D38V (8), W77R (9), R83C (4), R83H (6), E110K (3), E110Q (8), A124T (9), V166G (7), P178S (6), G184E (9), G188S (6), G188R (10), L211P (9), G222R (5), W236R (6), P257L (11), G270V (6), R295C (4), and L345R (6), were shown to abolish or greatly reduced G6Pase activity by site-directed mutagenesis and transient expression assays. In this study, we constructed

TABLE I
Mutations identified in the G6Pase gene of GSD-1a patients

Patient	Exon	Mutation	Effect on coding sequence	Comment
1	V	843C → T/T255I	Thr to Ile at 255	Homozygote
2	I	158delC	Frameshift, stop at 35	Compound heterozygote
	V	1118C → T/Q347X	Gln → Stop at 347	
3	I	288G → A/W70X	Trp → Stop at 70	Compound heterozygote
	V	836delA	Frameshift, stop at 300	
4	V	1057delTTC/ΔF327	Del Phe at 327	Homozygote

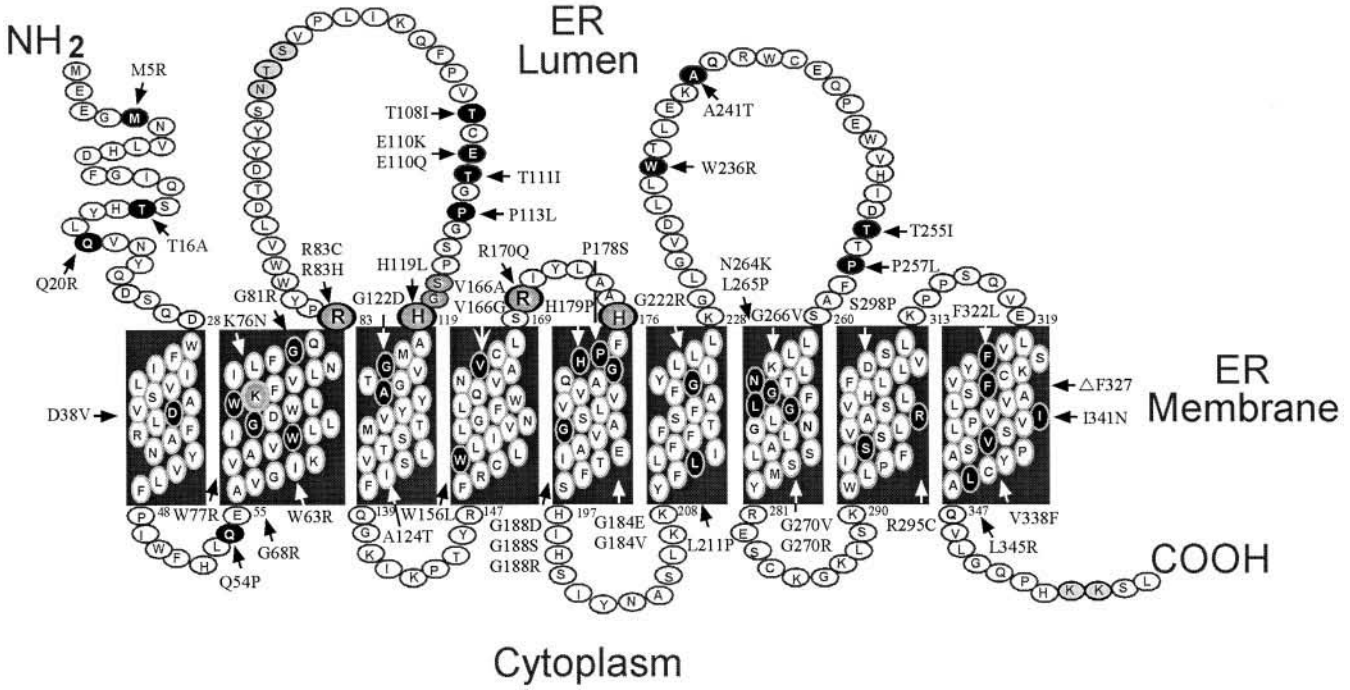

FIG. 1. **Location of missense and ΔF327 mutations identified in the *G6Pase* gene of GSD-1a patients.** Human G6Pase is anchored to the ER by nine transmembrane helices (18, 19). The mutations are indicated and shown in *black*. Amino acid residues comprising the phosphatase signature motif are denoted by *large shaded circles*.

35 mutants carrying G6Pase missense mutations, including 29 mutations that have not been characterized and 6 of the previously characterized mutations, W77R, A124T, G184E, L211P, G188R, and P257L. Glucose-6-phosphate hydrolytic activities of these mutants were examined after transient expression of WT or mutant G6Pase cDNA into COS-1 cells. We also included in this study the single codon deletion mutation, ΔF327, shown to be devoid of enzymatic activity (5). To facilitate structure-function analysis, we have grouped these mutations into three categories (active site, helical, and nonhelical mutations) based on their predicted catalytic, transmembrane helical, luminal, and cytoplasmic locations in G6Pase (Fig. 1).

The amino acids predicted to be critical to glucose-6-phosphate binding and hydrolysis include Lys^{76}, Arg^{83}, His^{119}, Arg^{170}, and His^{176} (12–14). Five active site mutations, K76N (16), R83C (4), R83H (6), H119L (17), and R170Q (15), have been identified in the *G6Pase* gene of GSD-1a patients. In earlier studies (4, 6), we have shown that R83C and R83H mutants were devoid of G6Pase activity (Table II). In this study, we demonstrate that K76N, H119L, and R170Q mutations also completely abolished phosphohydrolase activity (Table II), demonstrating the importance of these residues in G6Pase catalysis.

Twelve of the 13 nonhelical G6Pase mutations are situated inside the ER lumen, and 1 (Q54P) is located in cytoplasmic loop 1 (Fig. 1). Earlier studies have shown that the E110K (2) mutation totally inactivated G6Pase, but the E110Q (8), W236R (6), and P257L (11) mutations only markedly reduced

TABLE II
Phosphohydrolase activity of G6Pase active site mutant constructs

WT or mutant G6Pase construct was transfected into COS-1 cells, and phosphohydrolase activity was assayed as described under "Materials and Methods" using two independent isolates of each construct in three separate transfections. Data are presented as the mean ± S.E.

Mutation	Non-FLAG construct	3′ FLAG construct
	(nmol/min/mg)	*(nmol/min/mg)*
Mock	6.75 ± 0.28	11.99 ± 0.15
WT	69.42 ± 5.78	73.36 ± 1.82
K76N	5.44 ± 0.86	9.03 ± 0.68
R83C	6.32 ± 0.64	9.28 ± 0.24
R83H	5.18 ± 0.10	9.26 ± 0.90
H119L	6.32 ± 0.16	10.86 ± 0.84
R170Q	4.94 ± 0.07	8.61 ± 0.62

phosphatase activity. This was confirmed in the present study demonstrating that eight nonhelical mutants, M5R, T16A, E110Q, T111I, W236R, A241T, T255I, and P257L, retained residual phosphohydrolase activity (Table III). Four mutants, T16A, E110Q, T111I, and A241T, possessed ≥10% WT G6Pase activity. The five nonhelical mutations that completely abolished G6Pase activity include Q20R, Q54P, T108I, E110K, and P113L (Table III). Q20R and Q54P are located within the amino terminus and cytoplasmic loop 1, respectively, and E110K, T108I, and P113L are all situated within luminal loop 1 (Fig. 1).

Thirty missense mutations (excluding the active site mutation K76N in helix 2) and the ΔF327 mutation are scattered

TABLE III

Phosphohydrolase activity of G6Pase nonhelical mutant constructs

WT or mutant G6Pase construct was transfected into COS-1 cells, and phosphohydrolase activity was assayed as described under "Materials and Methods" using two independent isolates of each construct in three separate transfections. Data are presented as the mean ± S.E. Numbers in parentheses represent the percentage of WT enzymatic activity. N, amino-terminal domain; C, cytoplasmic loop; L, luminal loop.

Mutation	Location	Non-FLAG construct	3′ FLAG construct
		(nmol/min/mg)	*(nmol/min/mg)*
Mock		3.70 ± 0.48 (0)	12.00 ± 0.07 (0)
WT		93.03 ± 9.68 (100)	66.23 ± 3.44 (100)
M5R	N	12.57 ± 0.50 (9.9)	16.13 ± 0.88 (7.6)
T16A	N	23.81 ± 3.51 (22.5)	25.87 ± 0.69 (25.6)
Q20R	N	3.91 ± 0.35	10.38 ± 1.34
Q54P	C1	2.99 ± 0.27	10.85 ± 0.52
T108I	L1	2.37 ± 0.04	12.37 ± 0.53
E110K	L1	3.36 ± 0.01	10.52 ± 0.55
E110Q	L1	17.63 ± 1.03 (15.6)	21.00 ± 0.88 (16.6)
T111I	L1	16.77 ± 0.15 (14.6)	19.94 ± 0.72 (14.6)
P113L	L1	4.31 ± 0.14	11.47 ± 0.48
W236R	L3	8.31 ± 0.43 (5.2)	17.12 ± 0.42 (9.4)
A241T	L3	20.59 ± 1.36 (18.9)	24.80 ± 1.21 (23.6)
T255I	L3	5.96 ± 0.02 (2.5)	12.92 ± 1.33 (1.7)
P257L	L3	9.77 ± 1.32 (6.8)	14.91 ± 1.32 (5.4)

throughout the nine transmembrane helices (Fig. 1). Earlier mutational studies have shown that 13 helical mutations, including D38V, W77R, A124T, V166G, P178S, G184E, G188S, G188R, L211P, G270V, R295C, ΔF327, and L345R, completely abolished G6Pase activity, and 1 helical mutation, G222R, retained residual activity (reviewed in Refs. 2 and 3). In this study, we extended this analysis and showed that 22 helical mutations completely inactivated the enzyme (Table IV). The nine helical mutants that retain residual G6Pase activity include D38V, G122D, A124T, W156L, V166A, P178S, L211P, G222R, and F322L. It is interesting to note that only two mutants, G122D (helix 3) and F322L (helix 9), retained >10% WT G6Pase activity. Also, G122D and A124T are the only mutations identified in helix 3.

The Active Site and Nonhelical Residues Play No Essential Role in the Stability of G6Pase—Structure-function analyses of G6Pase would be greatly facilitated by specific antibodies to G6Pase. However, polyclonal antibodies to human G6Pase are not specific. As an alternative strategy to monitor biosynthesis of mutated G6Pase, we have constructed all 48 missense and the ΔF327 G6Pase mutants with the eight-amino acid FLAG marker peptide (DYKDDDDK) at their carboxyl termini. The FLAG tag does not interfere with the expression, stability, or activity of WT G6Pase and has been used successfully to tag human G6Pase (18, 19) for topological studies. G6Pase biosynthesis in COS-1 cells was examined by Western blot analysis using a monoclonal antibody against the FLAG epitope.

In WT construct-transfected COS-1 cells, polypeptides of 41 and 37 kDa, representing glycosylated and nonglycosylated G6Pase, were synthesized (Fig. 2*A*). In the presence of a glycosylation inhibitor, tunicamycin (32), only the 37-kDa nonglycosylated G6Pase was detected, confirming their identities. We have previously shown that both forms of G6Pase are enzymatically active and that the nonglycosylated G6Pase retains ~40% activity (19). Immunoblot analyses showed that the active site mutants, K76N, R83C, R83H, H119L, and R170Q (Fig. 2), as well as the 13 nonhelical mutants (Fig. 3) supported the synthesis of similar amounts of G6Pase proteins as the WT construct. The results suggest that amino acid residues that comprise the catalytic center and nonhelical regions of the enzyme do not play an essential role in the correct folding and stability of G6Pase. Whereas the 41-kDa glycoprotein was the major form in WT-transfected cells, the 37-kDa nonglycosylated G6Pase became the major form in M5R-, Q20R-, Q54P-, T108I-, and W236R-transfected cells, suggesting the accumulation of incompletely processed protein in G6Pase mutant-transfected cells.

TABLE IV

Phosphohydrolase activity of G6Pase helical mutant constructs

WT or mutant G6Pase construct was transfected into COS-1 cells, and phosphohydrolase activity was assayed as described under "Materials and Methods" using two independent isolates of each construct in three separate transfections. Data are presented as the mean ± S.E. Numbers in parentheses represent the percentage of WT enzymatic activity. H, helix.

Mutation	Location	Non-FLAG construct	3′ FLAG construct
		(nmol/min/mg)	*(nmol/min/mg)*
Mock		6.75 ± 0.28 (0)	11.97 ± 0.02 (0)
WT		69.42 ± 5.80 (100)	70.16 ± 1.98 (100)
D38V	H1	7.93 ± 0.33 (1.9)	13.78 ± 0.68 (3.1)
W63R	H2	6.80 ± 0.31	10.46 ± 1.41
G68R	H2	6.95 ± 0.24	10.78 ± 0.84
W77R	H2	7.24 ± 0.49	11.36 ± 0.48
G81R	H2	7.20 ± 0.18	11.73 ± 0.89
G122D	H3	20.77 ± 1.69 (22.4)	31.71 ± 2.51 (34)
A124T	H3	9.81 ± 0.59 (4.9)	17.68 ± 0.43 (9.8)
W156L	H4	8.08 ± 0.33 (2.1)	13.39 ± 0.41 (2.4)
V166A	H4	9.46 ± 0.06 (4.3)	14.63 ± 1.06 (4.6)
V166G	H4	5.78 ± 0.65	11.47 ± 0.87
P178S	H5	7.86 ± 0.10 (1.8)	12.61 ± 0.58 (1.1)
H179P	H5	5.45 ± 0.74	11.10 ± 0.10
G184E	H5	5.56 ± 0.57	9.18 ± 0.58
G184V	H5	4.43 ± 0.39	9.10 ± 0.56
G188D	H5	4.55 ± 0.82	9.79 ± 0.64
G188S	H5	6.25 ± 0.83	7.57 ± 0.59
G188R	H5	6.42 ± 0.38	10.40 ± 1.01
L211P	H6	12.29 ± 1.07 (8.8)	15.20 ± 1.16 (5.6)
G222R	H6	8.35 ± 0.93 (2.6)	13.46 ± 1.31 (2.6)
N264K	H7	6.62 ± 0.07	11.73 ± 0.85
L265P	H7	5.29 ± 0.42	10.07 ± 0.50
G266V	H7	5.96 ± 0.57	9.50 ± 0.64
G270V	H7	5.42 ± 0.43	10.82 ± 1.05
G270R	H7	5.42 ± 0.21	11.32 ± 0.77
R295C	H8	5.97 ± 0.63	12.42 ± 0.95
S298P	H8	4.56 ± 0.27	11.98 ± 0.48
F322L	H9	15.70 ± 0.10 (14.3)	23.84 ± 1.55 (20.4)
ΔF327	H9	5.57 ± 0.40	11.57 ± 0.62
V338F	H9	4.71 ± 0.02	11.27 ± 1.27
I341N	H9	5.50 ± 0.43	11.11 ± 0.74
L345R	H9	5.63 ± 0.33	10.86 ± 0.31

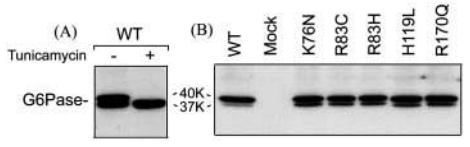

FIG. 2. **Western blot analysis of G6Pase in COS-1 cells transfected with WT or an active site mutant cDNA construct containing a 3′ FLAG tag.** *A*, effects of tunicamycin. COS-1 cells transfected with the G6Pase-WT construct were incubated in the absence or presence of tunicamycin (1 μg/ml) for 24 h before harvesting for Western blot analysis. *B*, Western blot analysis of active site mutants. Mock-transfected cells were used as controls. The G6Pase proteins on the Western membranes were visualized by an anti-FLAG monoclonal antibody; each lane contained 20 μg of proteins.

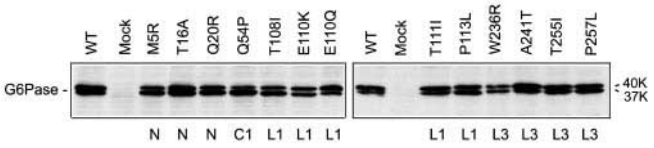

FIG. 3. **Western blot analysis of G6Pase in COS-1 cells transfected with WT or a nonhelical mutant cDNA construct containing a 3′ FLAG tag.** Mock-transfected cells were used as controls. The G6Pase proteins on the Western membranes were visualized by an anti-FLAG monoclonal antibody; each lane contained 20 μg of proteins.

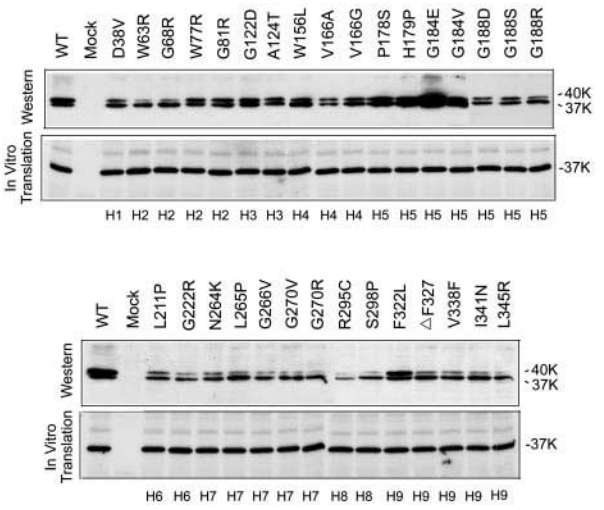

FIG. 4. **Synthesis of WT or helical G6Pase mutant analyzed by Western blot hybridization or by *in vitro* transcription-translation.** For Western blot analysis, COS-1 cells were transfected with WT or a helical G6Pase mutant cDNA construct containing a 3′ FLAG tag. Mock-transfected cells were used as controls. The G6Pase proteins on the Western membranes were visualized by an anti-FLAG monoclonal antibody; each lane contained 20 μg of proteins. For *in vitro* transcription-translation analysis, *in vitro* synthesis of G6Pase directed by 3′ FLAG-tagged WT or a mutant G6Pase construct in a pGEM-11Zf(+) vector was performed using the troponin T-coupled reticulocyte lysate system. L-[^{35}S]Methionine was used as the labeled precursor, and after electrophoresis, the proteins were visualized by fluoroautoradiography.

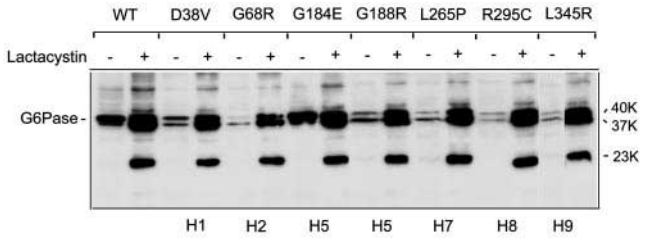

FIG. 5. **The effect of the proteasome inhibitor lactacystin on degradation of G6Pase.** Two sets of COS-1 cells were transfected with 3′ FLAG-tagged WT and mutant G6Pase constructs. After 34 h of incubation at 37 °C, 10 μM lactacystin was added to one set of cultures, and the incubation was continued for an additional 12–14 h. The steady-state levels of G6Pase in transfected cultures were examined by Western blot analysis using an anti-FLAG monoclonal antibody; each lane contained 20 μg of proteins.

The FLAG-tagged active site mutants, like the respective parental constructs, were devoid of G6Pase activity (Table II). Similarly, comparable amounts of phosphohydrolase activities were obtained with the tagged and nontagged G6Pase nonhelical mutants (Table III). Again, Q20R, Q54P, T108I, E110K, and P113L are the only nonhelical mutations that completely abolished G6Pase activity.

The Structural Integrity of Transmembrane Helices Is Vital to the Stability of G6Pase—The majority (64.5%) of helical mutants, including D38V (*H1*), W63R/G68R (*H2*), V166A (*H4*), G188D/G188S/G188R (*H5*), L211P/G222R (*H6*), N264K/L265P/G266V/G270V/G270R (*H7*), R295C/S298P (*H8*), and ΔF327/V338F/I341N/L345R (*H9*), supported the synthesis of reduced levels of G6Pase proteins in COS-1 cells as compared with the WT construct (Fig. 4). Moreover, the 41-kDa G6Pase was preferentially reduced, indicating that mutations that altered the structural integrity of transmembrane helices destabilize G6Pase. Interestingly, the steady-state level of the G184E mutant, which is devoid of G6Pase activity, was higher than that of WT G6Pase, suggesting that the G184E mutation increased the stability of this phosphatase.

Northern blot analysis confirmed that similar levels of G6Pase transcripts were expressed in WT or mutant G6Pase-transfected COS-1 cells (data not shown). Our results, therefore, demonstrate that the decrease in G6Pase biosynthesis was not due to a decrease in efficiency of expression of the transfected cDNA construct. Moreover, the helical mutant constructs, like WT G6Pase, directed the synthesis of similar amounts of G6Pase proteins in a cell-free transcription-translation system (Fig. 4). The results indicate that transmembrane helices in G6Pase play a vital role in the correct folding of the enzyme and that the abnormal mutant proteins are rapidly degraded in the cell.

Comparable amounts of G6Pase activities were obtained with FLAG-tagged or nontagged G6Pase helical mutants (Table IV). Again, 22 of the 31 helical mutants were devoid of enzymatic activity, and 9 mutants (D38V, G122D, A124T, W156L, V166A, P178S, L211P, G222R, and F322L) retained residual G6Pase activity.

The Proteasome Inhibitor Lactacystin Induces the Accumulation of WT and Mutant G6Pase—The effect of a proteasome inhibitor, lactacystin (26), on steady-state levels of G6Pase was assessed by immunoblot analysis of COS-1 cells transfected with WT or mutant G6Pase construct. In WT-transfected cells, the steady-state levels of both 41-kDa and 37-kDa G6Pases were markedly increased in the presence of lactacystin (Fig. 5), indicating that G6Pase is predominantly degraded in cells through the proteasome pathway. Lactacystin inhibits degradation of both glycosylated and nonglycosylated G6Pases, suggesting that this metabolite does not inhibit the processing and maturation of G6Pase. In the presence of lactacystin, a fast-migrating band of 23 kDa was also accumulated (Fig. 5). The nature of this polypeptide is unknown. It is also unclear whether additional intermediates are accumulated in the presence of lactacystin because the antibody recognizes the FLAG tag at the carboxyl terminus of the enzyme.

In the absence of lactacystin, the steady-state levels of mutant proteins in D38V-, G68R-, G188R-, L265P-, R295C-, and L345R-transfected cells were lower than that in WT G6Pase-transfected cells (Fig. 5). However, in the presence of lactacystin, a marked increase in the accumulation of both the 41- and 37-kDa mutant G6Pases comparable to that of WT G6Pase was observed (Fig. 5), indicating that proteasomes also participate in the degradation of G6Pase mutants. In the absence of lactacystin, the G184E construct supported the synthesis of increased levels of G6Pase protein rather than that of WT construct. In the presence of lactacystin, comparable amounts of G184E and WT G6Pase were accumulated (Fig. 5), again suggesting that the G184E mutation increased the stability of G6Pase.

DISCUSSION

Human G6Pase is anchored to the ER by nine transmembrane helices with the amino terminus and catalytic center facing inward in the lumen and the carboxyl terminus facing outward in the cytoplasm (18, 19). In this study, we examined phosphohydrolase activities of G6Pase mutants carrying 48 missense mutations and the ΔF327 codon deletion mutation grouped into three categories based on their predicted catalytic, helical, and nonhelical locations in this phosphatase. We have also undertaken structure-function analysis of human G6Pase. We show that mutations that altered the active center in G6Pase completely inactivated the enzyme but had no deleterious effects on the folding and stability of the protein. Eight of the 13 nonhelical mutants retained residual G6Pase activity, and most, it not all, supported the synthesis of WT levels of G6Pase protein in COS-1 cells, suggesting that nonhelical mu-

tants also play no essential role in the stability of G6Pase. On the other hand, of the 31 helical mutations characterized, 22 (71%) completely abolished G6Pase activity, and 20 (64%) destabilized this phosphatase. Taken together, the results indicate that the structural integrity of transmembrane helices is vital to the stability and enzymatic activity of G6Pase. We have also provided evidence indicating that G6Pase is degraded predominantly through the proteasome pathway.

Based on the crystal structure of vanadium-containing chloroperoxidase (13, 14), the amino acids predicted to participate in G6Pase catalysis include Lys^{76}, Arg^{83}, His^{119}, Arg^{170}, and His^{176}. As expected, the five active site mutations, K76N, R83C, R83H, H119L, and R170Q, completely inactivated the enzyme, confirming the importance of these residues in G6Pase catalysis. Whereas 22 of the 31 (71%) helical mutations completely abolished G6Pase activity, only 5 of the 13 (38%) nonhelical mutants were devoid of enzymatic activity, suggesting that an active G6Pase depends upon the structural integrity of its transmembrane helices. Luminal loop 1 may also play a crucial role in catalytic activity of the enzyme because T108I, E110K, and P113L mutations, which totally inactivated G6Pase, are located within this loop. The nine helical mutants that retain residual G6Pase activity include D38V, G122D, A124T, W156L, V166A, P178S, L211P, G222R, and F322L. Earlier studies have shown that D38V (8), P178S (6), and A124T (9) mutants were devoid of G6Pase activity. The observed difference may result from the low levels of G6Pase activity retained by these mutants. Currently, we are adapting a recombinant adenoviral vector-mediated expression system, which has been widely used for high-level protein expression in mammalian cells (33), to increase the sensitivity of the expression assays.

It is interesting to note that a Japanese patient homozygous for the P257L mutation, a nonhelical mutation that only partially inactivates G6Pase, had a very mild phenotype (11). The patient experienced no hypoglycemic episodes and required no dietary therapy. The data base of residual phosphohydrolase activity retained by the 49 G6Pase codon mutants should facilitate future genotype-phenotype delineations. It is important to document the results of phenotypic studies of GSD-1a patients carrying leaky *G6Pase* mutations. Knowledge of the minimal G6Pase activity needed to prevent hypoglycemic episodes in GSD-1a patients will facilitate the development of novel therapeutic approaches for this disorder.

Virtually nothing is known about the structural requirements for the correct folding and stability of G6Pase. We therefore undertook structure-function analyses of this phosphatase, taking advantage of the large collection of *G6Pase* missense mutations identified in GSD-1a patients. We show that amino acid residues comprised of the active center and nonhelical regions of G6Pase played no essential role in the stability of the protein. On the other hand, evidence present in this study indicates that the structural integrity of transmembrane helices is vital to the correct folding and stability G6Pase. Immunoblot analysis demonstrate that whereas all active site and nonhelical mutants supported the synthesis of WT levels of G6Pase protein in COS-1 cells, 20 of the 31 (64%) helical mutants supported the synthesis of reduced levels of G6Pase as compared with the WT construct. In a cell-free translation system, WT and the helical mutant transcripts direct the synthesis of similar amounts of G6Pase proteins. Because folding of nascent proteins occurs during their *in vitro* synthesis on rabbit reticulocyte ribosomes, our data strongly suggest that mutations that alter the helical structure in G6Pase cause misfolding and degradation of the mutant protein.

Proteins with abnormal conformations that arise by mutations or intracellular denaturation are rapidly degraded, which represents a quality control system in the cell (20, 34). Most intracellular protein degradation is catalyzed by lysosomal proteases or the ubiquitin-proteasome system (reviewed in Ref. 24). Many membrane proteins, including cystic fibrosis transmembrane conductance regulator (21, 22), the major histocompatibility complex class I molecule, and α-chains of T-cell antigen receptor, are degraded in cells by the proteasome system (reviewed in Refs. 23–25). The 26S proteasome, an ATP-dependent proteolytic complex, contains the central 20S proteasome, in which proteins are degraded, and two 19S complexes, which provide substrate specificity and regulation (reviewed in Refs. 23–25). The active site nucleophil of the proteasome is the hydroxyl group of a threonine at the amino terminus of the β subunit of proteasome. Lactacystin, a specific proteasome inhibitor, blocks proteasome function by becoming covalently linked to the hydroxyl group of threonine (26, 27). In this study, we show that the steady-state levels of WT and mutant G6Pase were markedly increased by lactacystin, indicating that degradation of G6Pase is mediated predominantly by the proteasome pathway. The marked increase in the levels of WT G6Pase by lactacystin suggests that folding of G6Pase is relatively inefficient, a phenomenon also observed for the cystic fibrosis transmembrane conductance regulator (35, 36).

In summary, we have generated a data base of residual G6Pase activity retained by 49 codon mutations to facilitate genotype-phenotype delineation, elucidated a number of structural requirements for the stability and enzymatic activity of G6Pase, and demonstrated that proteasomes mediate degradation of this phosphatase.

REFERENCES

1. Chen, Y.-T. (2001) in *The Metabolic and Molecular Bases of Inherited Disease* (Scriver, C. R., Beaudet, A. L., Sly, W. S., Valle, D., Childs, B., Kinzler, K. W., and Vogelstein, B., eds) 8th Ed., pp. 1521–1551, McGraw-Hill Inc., New York
2. Chou, J. Y., and Mansfield, B. C. (1999) *Trends Endocrinol. Metab.* **10,** 104–113
3. Chou, J. Y. (2001) *Curr. Mol. Med.* **1,** 25–44
4. Lei, K.-J., Shelly, L. L., Pan, C.-J., Sidbury, J. B., and Chou, J. Y. (1993) *Science* **262,** 580–583
5. Lei, K.-J., Shelly, L. L., Lin, B., Sidbury, J. B., Chen, Y.-T., Nordlie, R. C., and Chou, J. Y. (1995) *J. Clin. Invest.* **95,** 234–240
6. Lei, K.-J., Chen, Y.-T., Chen, H., Wong, L.-J. C., Liu, J.-L., McConkie-Rosell, A., Van Hove, J. L. K., Ou, H. C.-Y., Yeh, N. J., Pan, L. Y., and Chou, J. Y. (1995) *Am. J. Hum. Genet.* **57,** 766–771
7. Parvari, R., Lei, K.-J., Bashan, N., Hershkovitz, E., Korman, S. H., Barash, V., Lerman-Sagie, T., Mandel, H., Chou, J. Y., and Moses, S. W. (1997) *Am. J. Med. Genet.* **72,** 286–290
8. Parvari, R., Lei, K.-J., Szonyi, L., Narkis, G., Moses, S., and Chou, J. Y. (1997) *Eur. J. Hum. Genet.* **5,** 191–195
9. Bruni, N., Rajas, F., Montano, S., Chevalier-Porst, F., Maire, I., and Mithieux, G. (1999) *Ann. Hum. Genet.* **63,** 141–146
10. Weston, B. W., Lin, J. L., Muenzer, J., Cameron, H. S., Arnold, R. R., Seydewitz, H. H., Mayatepek, E., Van Schaftingen, E., Veiga-da-Cunha, M., Matern, D., and Chen, Y. T. (2000) *Pediat. Res.* **48,** 329–334
11. Akanuma, J., Nishigaki, T., Fujii, K., Matsubara, Y., Inui, K., Takahashi, K., Kure, S., Suzuki, Y., Ohura, T., Miyabayashi, S., Ogawa, E., Iinuma, K., Okada, S., and Narisawa, K. (2000) *Am. J. Med. Genet.* **91,** 107–112
12. Stukey, J., and Carman, G. M. (1997) *Protein Sci.* **6,** 469–472
13. Hemrika, W., and Wever, R. (1997) *FEBS Lett.* **409,** 317–319
14. Hemrika, W., Renirie, R., Dekker, H. L., Barnett, P., and Wever, R. (1997) *Proc. Natl. Acad. Sci. U. S. A.* **94,** 2145–2149
15. Huner, G., Podskarbi, T., Schutz, M., Baykal, T., Sarbat, G., Shin, Y. S., and Demirkol, M. (1998) *J. Inherit. Metab. Dis.* **21,** 445–446
16. Kozak, L., Francova, H., Hirabincova, E., Stastna, S., Peskova, K., and Elleder, M. (2000) *Hum. Mutat.* **16,** 89
17. Wu, M.-C., Tsai, F.-J., Lee, C.-C., Tsai, C.-H., and Wu, J.-Y. (2000) *Hum. Mutat.* **16,** 447
18. Pan, C.-J., Lei, K.-J., Annabi, B., Hemrika, W., and Chou, J. Y. (1998) *J. Biol. Chem.* **273,** 6144–6148
19. Pan, C.-J., Lei, K.-J., and Chou, J. Y. (1998) *J. Biol. Chem.* **273,** 21658–21662
20. Wickner, S., Maurizi, M. R., and Gottesman, S. (1999) *Science* **286,** 1888–1893
21. Ward, C. L., Omura, S., and Kopito, R. R. (1995) *Cell* **83,** 121–127
22. Jensen, T. J., Loo, M. A., Pind, S., Williams, D. B., Goldberg, A. L., and Riordan, J. R. (1995) *Cell* **83,** 129–135
23. Brodsky, J. L., and McCracken A. A. (1997) *Trends Cell Biol.* **7,** 151–156
24. Lee, D. H., and Goldberg, A. L. (1998) *Trends Cell Biol.* **8,** 397–403
25. Lecker, S. H., Solomon, V., Mitch, W. E., and Goldberg, A. L. (1999) *J. Nutr.* **129,** 227S–237S

26. Fenteany, G., Standaert, R. F., Lane, W. S., Choi, S., Corey, E. J., and Schreiber, S. L. (1995) *Science* **268,** 726–731
27. Fenteany, G., and Schriber, S. L. (1998) *J. Biol. Chem.* **273,** 8545–8548
28. Orita, M., Iwahana, H., Kanazawa, H., Hayashi, K., and Sekiya, T. (1989) *Proc. Natl. Acad. Sci. U. S. A.* **86,** 2766–2770
29. Lei, K.-J., Shelly, L. L., Pan, C.-J., Liu, J.-L., and Chou, J. Y. (1995) *J. Biol. Chem.* **270,** 11882–11886
30. Ausubel, F. M., Brent, R., Kingston, R. E., Moore, D. D., Seidman, J. G., Smith, J. A., and Struhl, K. (1992) *Current Protocols in Molecular Biology*, pp. 9.2.1–9.2.6, Greene Publishing and Wiley-Interscience, New York
31. Hers, H. G. (1964) in *Advances in Metabolic Disorders* (Levine, R., and Luft, L., eds), Vol. 1, pp. 1–44, Academic Press, London
32. Struck, D. K., and Lennarz, W. J. (1977) *J. Biol. Chem.* **252,** 1007–1013
33. Antinozzi, P. A., Berman, H. K., O'Doherty, R. M, and Newgard, C. B. (1999) *Annu. Rev. Nutr.* **19,** 511–544
34. Bross, P., Corydon, T. J., Andersen, B. S., Jorgensen M. M., Bolund, L., and Gregersen, N. (1999*) Hum. Mutat.* **14,** 186–198
35. Cheng, S. H., Gregory, R. J., Marshall, J., Paul, S., Souza, D. W., White, G. A., O'Riordan, C. R., and Smith, A. E. (1990) *Cell* **63,** 827–834
36. Kopito, R. R. (1999) *Physiol. Rev.* **79,** S167–S173